論文 / 著書情報
Article / Book Information

Title	Molecular dynamics study of nano-porous materials—Enhancement of mobility of Liions in lithium disilicate
Authors	Junko Habasaki
Citation	J. Chem. Phys, 145, , 204503
Pub. date	2016, 11
Note	This article may be downloaded for personal use only. Any other use requires prior permission of the author and AIP Publishing. The following article appeared in J. Chem. Phys, 145, , 204503 and may be found at http://dx.doi.org/10.1063/1.4967874.

AIP | The Journal of Chemical Physics

Molecular dynamics study of nano-porous materials—Enhancement of mobility of Li ions in lithium disilicate

Junko Habasaki

Citation: The Journal of Chemical Physics **145**, 204503 (2016); doi: 10.1063/1.4967874
View online: http://dx.doi.org/10.1063/1.4967874
View Table of Contents: http://scitation.aip.org/content/aip/journal/jcp/145/20?ver=pdfcov
Published by the AIP Publishing

Molecular dynamics study of nano-porous materials—Enhancement of mobility of Li ions in lithium disilicate

Junko Habasaki[a)]
School of Materials and Chemical Technology, Tokyo Institute of Technology, Nagatsuta 4259, Yokohama 226-8502, Japan

(Received 17 August 2016; accepted 3 November 2016; published online 22 November 2016)

In several nano-porous materials and their composites, enhancement of ionic conductivity has been reported and several mechanisms having different origins have been proposed so far. In the present work, ionic motion of Li ions in porous lithium disilicates is examined by molecular dynamics simulation in the constant volume conditions and the enhancement of the dynamics is predicted. Structures and dynamics of ions in a nano-porous system were characterized and visualized to clarify the mechanism of the enhancement. The diffusion coefficient of Li ions has shown the maximum in the medium density (and porosity) region, and near the maximum, shortening of the nearly constant loss region in the mean squared displacement of ions as well as changes of the structures of the coordination polyhedra, LiO_x is found. It suggests that the loosening of the cage, which increases the jump rate of ions, is an origin of the enhancement. When larger (but still in a nano-scale) voids are formed with a further decrease of density, more tight cages are reconstructed and the diffusion coefficient decreases again. These behaviors are closely related to the residual stress in the system. It is noteworthy that the explanation is not based on the percolation of the path only or formation of boundaries, although the former also affects the dynamics. *Published by AIP Publishing.* [http://dx.doi.org/10.1063/1.4967874]

I. INTRODUCTION

Recently, porous materials play important roles in the nano-technology. They are the candidates of the useful electric devices, such as electrode, which can show high performance. All solid-state lithium batteries based on the porous system are proposed[1–3] and it is beneficial to reduce the weight of the battery with maintaining a good quality. Thus application of porous materials to such fields is promising.

Interestingly, enhancement of the dynamics (or an opposite case) has been reported for several porous systems and/or related composites.[4–15] To explain the mechanism of the enhancement, several scenarios having different origins have been suggested. So far, concepts of charge transfer and space charge effects[7,8] and the effect of epitaxial strain in opening diffusion paths[12] were proposed. Influence of atomic and electronic reconstruction at the interface in stabilizing new phases with increased carrier concentration[13,14] was also suggested.

Although almost all of these explanations are related to the characters of the boundaries, question remains for the role of nano-particles and/or nano-porous materials. For better understanding of the mechanism of the enhancement of the dynamics in a nano-porous system, molecular dynamics (MD) simulation has been performed in the present work.

So far, lithium disilicate in the molten, glassy, crystalline states has been examined successfully from many points of views by several groups,[16–24] where our potential model (force field) previously developed based on the *ab initio* MO calculations[24] was commonly used. Since the model covers a wide range of potential surfaces, it will be useful for further systematical comparison of systems with different states including porous ones. Therefore, in the present work, porous lithium disilicate systems are chosen for the examination of structures and dynamics as typical nano-porous ionic systems.

In some porous crystalline systems, contribution of disorder for the enhancement is pointed out and it is useful to separate the role of disorder from other factors beforehand. In the present work, the system in the glassy state is used as the starting materials before introducing pores. A comparison of crystalline and glassy lithium disilicates reveals that the latter has a diffusion coefficient (and hence conductivity) of several orders larger than the former as shown by both experiment[25] and simulations.[22] Similar trends are also known for other systems,[26,27] for which both the crystalline and glassy states were examined. Therefore, the effects of disorder are well separated from other factors in the present model.

In these decades, several methods to prepare the porous silica in the MD simulations were proposed. We have applied one of these methods to prepare the porous lithium disilicate systems with different densities. Then dynamics and related structures of these systems were examined. It was predicted that there is the maximum of the diffusion coefficient when the density of the system is decreased. By further analyses, it is found that the change in the caging of ions contributes it and the geometrical correlations of the walks of ions modify the behaviors. Characteristics of the caged ion dynamics have been examined on the basis of the concept of a geometrical degree of the freedom[28] of the polyhedra formed by oxygen atoms around lithium ions[29,30] and systems. Similar analysis was recently successfully applied on ionic liquid[31] to characterize the glass transition of it. The dynamics of

a)Author to whom correspondence should be addressed. Electronic mail: habasaki.j.aa@m.titech.ac.jp

caged ions are comparable to the caged particles near the glass transition temperature, and the explanation for the enhanced dynamics in porous materials is worth to discuss in relation with the mechanism of the slowing down of the dynamics by caging near T_g. Therefore, the nano-ionics in the porous materials is an interesting problem not only for the nano-technology but also for a fundamental research field to understand the complex ion dynamics and its relation to the glass transition.[15]

II. METHODS

A. MD simulations

In the present work, porous systems were prepared by the scaling of the volume and position of particles at 600 K and the resultant density is changed from 1.0 to 0.64 times of a original (glassy lithium disilicate before the expansion) system. Similar methods are previously used to prepare the porous silica[32,33] as will be explained later.

Each original and porous lithium disilicate ($Li_2Si_2O_5$) system examined contains 768 Li ions, 768 Si atoms, and 1920 O atoms in the basic MD box with a periodic boundary condition. The following model function was used:

$$\phi_{ij} = \frac{z_i z_j e^2}{r} + f_0(b_i + b_j)\exp\left(\frac{a_i + a_j - r}{b_i + b_j}\right) - c_i c_j r^{-6}. \quad (1)$$

The model consists of the Coulombic term, the pair potential function of Gilbert–Ida type[34,35] with the r^{-6} for the correction of the softness of the oxygen atom. Potential parameters were previously obtained from the *ab initio* MO calculations[24] for silicates such as Li, Na, and K salts by us. The value r is the distance between atoms, a_i is the effective radius, and b_i is the softness parameter of the atom i with a constant f_0(=1 kcal Å^{-1} mol^{-1} = 4.184 kJ Å^{-1} mol^{-1}). The Ewald method was used for the calculation of Coulombic force. A cutoff distance of the calculation of repulsive force and that for the real space of the Coulombic term were chosen to be 12 Å throughout the present work.

Lithium disilicate in the glassy state was obtained by the rapid cooling (~1 K ps^{-1}) from the melt at 3000 K with the combination of a constant pressure condition and temperature scaling to the target temperatures (2500, 2000, 1700, 1400, 1000, 800, 700, and 600). Systems were quasi-equilibrated at each temperature in the NVT condition followed by the NVE condition. The time step used in the MD run was changed according to the diffusivity of the system. It was chosen to be 1 fs for $T > 800$ K and 4 fs for $T \leq 800$ K for the original system, while the former value was used for almost porous systems. For the original system, the computational glass transition temperature is at around 1000 K. Motion of the frameworks is negligibly small during the MD run of several ns below this temperature. The diffusivity and/or viscosity of the simulated system using our potential model is reported[19] to be comparable to the experiments in several conditions, and therefore T_g located between 720 and 800 K is expected for the longer runs.

B. Quality of the potential model

So far, the model has been successfully applied for melts and glasses by several groups.[16–23] Stability of the crystals under the constant pressure condition is a strict check of the quality of the potential model. Our potential model based on the *ab initio* MO calculation has been tested[24,36] for several polymorphs of crystals under the constant pressure conditions (in the atmospheric condition) as well as melts and glasses. Since the comparison with experimentally obtained dynamics is successful,[15,19,37] the model well covers different states of the lithium silicates. Therefore, it is suitable to examine the fundamental mechanism of the enhancement and comparison of systems in different states, even though it was not optimized for porous materials. If it is necessary, the porous system thus prepared can be used as an input for the further examination of the system by *ab initio* MD or related methods.

In the present work, MD runs were performed by using the Verlet algorithm, which is known to be a symplectic integrator. The numerical error in the solution of the equation of the motion itself is small enough to keep the energy of the system in the NVE condition. A standard deviation of the total energy is found to be less than 5×10^{-4} of the total energy at 800 K, during 12 ns runs.

C. Preparation of porous model for simulations

There are several methods to prepare porous models for MD (or MC) simulations. Kieffer and Angell[32] prepared porous silica by the expansion of the dense silica system. The method is later refined by Nakano *et al.*[33] A different method, a charge scaling procedure, was applied for the preparation of a nano-porous silica model by Beckers and De Leeuw.[38] The porous system also can be prepared by the aggregation process. Bhattacharya and Kieffer[39] used a reaction force field to examine it which is formed by silicic acid in water. Recently, Habasaki and Ishikawa[40] prepared a porous system based on the spontaneous formation of gel from a colloidal system, which consists of silica nano-colloids, water, and salt. Although the structures prepared by different methods are not necessarily the same,[41] common tendencies by introducing pores are expected.

In the present work, the method, by the expansion of the system and coordinate (with some modifications), was applied for preparing the porous lithium disilicate systems with different densities. That is, an expansion of the system, by scaling of factor 1.005 times (for both axis length and coordinate), was repeated every 3000 time steps until the density to be examined was obtained. The densities ρ examined are 2.47 (original), 2.30, 2.13, 1.98, 1.84, and 1.58 (density is given in g cm^{-1} throughout this work). Experimental density of the system in the glassy state was reported to be 2.35.[42] After the expansion of the system, each system was equilibrated during 300 000 steps run in the *NVT* condition. Then further 300 000 steps run was done in the NVE condition. If the temperature increased during the *NVE* run (due to the non-equilibrium nature of the system), short *NVT* runs (~30 000 steps using a Gaussian thermostat) were inserted between *NVE* runs. The run for 300 000–4 000 000 steps, which was performed in the *NVE* condition after the equilibration, was used

for further analysis. For temperature dependence of the dynamics (600-1000 K) in porous materials, simulations have been started from the porous systems at 600 K and the same system volume was used at each target temperature. For the system with ρ = 1.98 and 1.58 at 600 K, an additional *NPT* run has been done after the *NVE* run to check the effects of residual stress in the system.

III. RESULTS AND DISCUSSION

A. Relation between porosity and density

Porosity (the ratio of the volume of space to the total volume, that is, the fraction of void), P_o (in %) was obtained from MD simulations (after equilibration at each density) for each density, ρ (in g cm^{-3}) of the original and porous systems. For the systems with ρ = 2.47, 2.13, 1.98, 1.84, and 1.58 at 600 K, porosities are determined to be, 56.62, 62.59, 65.34, 67.80, and 72.29, respectively. These values were determined by geometric considerations using the ionic radius.[43] (Here we used Si: 0.40, O: 1.21, and Li: 0.9 as ionic radii which are consistent to the maximum position of the first peak of g(r) for Si–O (1.63 in original system at 600 K) and Li–O (2.04 in original system at 600 K) pairs.) (Lengths are given in Å throughout the present work.) In this method, overlaps of neighboring particles are taken into account. Therefore, the method is not for an "available space" but for the "precise amount of free space."[43] This method may not be suitable for cases with multi-neighbor intersections; however, it is applicable to the porous materials without a serious problem because of small overlaps. The porosity, P_o was found to be proportional to −ρ and hence the results are shown as the function of the density

$$\mathrm{Po} = -17.57(\rho/1000) + 100.08\ . \tag{2}$$

Therefore, results related to the different porosities of the systems will be shown as the function of the density in the present work. It is noteworthy that this relation holds including the case of ρ = 1.58, where the larger (but still in a nano-scale) voids are formed in the system. It means that the total amount of free volume is kept unchanged during the rearrangement of structures after the formation of such voids.

B. Comparison of mean squared displacement (MSD) of Li ions in the porous and original systems

To consider the origin of changes of diffusivity (or conductivity) with porosities, time developments of MSD of systems with different densities were examined.

The mean squared displacement (MSD) of ions or atoms can be obtained from the MD simulations data using the following relations:

$$\left\langle r^2(t)\right\rangle = \left\langle \left\{ \sum_{i=1}^{N_i} \left(r_i(t) - r_i(0)\right)^2 \right\} / N_i \right\rangle . \tag{3}$$

Four distinct time regions for MSD of Li ions in the original (before expansion) $Li_2Si_2O_5$ system in the glassy state at 800 K are explained as follows. These regions are shown in the upper panel of Figure 1 for the data of Li ions at 600 K and 800 K. MSDs of Si and O atoms at 600 K and 800 K are also shown in the lower panel. Previously, characterization of the motions

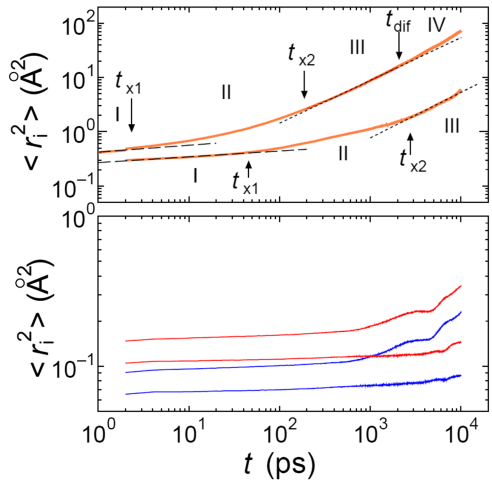

FIG. 1. Top: MSD of Li ions in original lithium disilicate glass at 600 K (lower curve) and 800 K (upper curve). Dashed and dotted lines (fitted to power laws) for Li ions at each temperature are for NCL and power law regions, respectively. Bottom: MSD of Si (blue curves) and O (red curves) at both temperatures. At 600 K, nearly flat (NCL) region is expanded to ~30 ps and power law region starts at ~3 ns. Flat region of MSD for Si and O continues up to ~ns at both temperatures.

of Li ions in each time region has been done with the help of van Hove functions, fractal dimension of random walks, and intermediate scattering functions for lithium silicate systems with several compositions[15,16,18] and is summarized below.

Region I (NCL): After the initial increase of MSD (in this figure, the short time region <1 ps for Li ion at 800 K and the region <2 ps for other cases are omitted) due to the local motion of ion site, a nearly flat region assigned to the nearly constant loss (NCL) is found. This time region is located between approximately 0.2 ps and 2 ps where the MSD increases with time as t^{α} with $\alpha \approx 0.07$. In this time region, ions are still caged by surrounding oxygen atoms and further shells of ions and atoms. If the time region becomes longer, it means that the cage is tight, while if the region becomes shorter, it means that the caging is loose and jump motions to the next shell begin. Therefore, the length of this time region is related to the jump rate of the caged ion.

Region II: Primitive jump is found in this region, where the MSD rises more rapidly than t^{α} of regime (I). In this intermediate time regime of about $t_{x1} < t < t_{x2}$, MSD is nearly proportional to time and this statement can be easily confirmed by the linear scale plot.

Region III: Power law behaviors of MSD are found in the region $t_{x2} < t < t_{dif}$. That is, MSD depends on t^{θ} with θ<1. Both fast and slow ions are found here and the slope θ is affected by the back-correlated motion of jumps considerably in the glass.

The exponent θ is a function of the fractal dimension of the random walk,[44] d_w, which is an index to represent the complexity of trajectories.

For the mean behavior of fast and slow ions,[18,44,45]

$$\theta = 2/d_w\ . \tag{4}$$

Region IV: Diffusive region of ions is found after t_{dif}, where MSD reaches to the square of the typical neighboring distance of ion sites and the MSD shows a linear t dependence in that region. With decreasing temperature, each time region becomes longer and longer. Namely, the diffusive regime is

found after 2 ns at 800 K for Li ions, while it is found after ~15 ns at 600 K.

Both Si and O atoms shown in the lower panel of Figure 1 are immobile for a long time. That is, the motion of the SiO_4 network in the original glass is negligibly small. A slight increase of the mobility for these species is found at ~1 ns at 800 K.

From the slope after t_{dif}, the diffusion coefficient of ions can be determined by the following Einstein equations:[46]

$$D = \frac{1}{6}\lim_{t\to\infty}\frac{d}{dt}\left\langle[\mathbf{r}_i(t) - \mathbf{r}_i(0)]^2\right\rangle. \quad (5)$$

The complex conductivity $\sigma^*(\omega)$ is related to the MSD by the following equation:[47,48]

$$\sigma^*(\omega) = -\omega^2\frac{N_\rho q_c^2}{6H_R kT}\int_0^\infty \left\langle r^2(t)\right\rangle e^{-i\omega t}dt, \quad (6)$$

where N_ρ is a number density of mobile ions, q_c is a charge of ions, k is the Boltzmann constant, H_R is the Haven ratio, and T is the temperature. Using this relation, the $\sigma^*(\omega)$ spectra in frequency domain can be connected to the motion in each stage of MSD in time domain. The Haven ratio[49] can be experimentally obtained from the ratio of tracer diffusion and conductivity. It can be represented by the ratio, $\sum_i \langle \mathbf{v}_i(0)\cdot\mathbf{v}_i(t)\rangle / \left\langle \sum_i \mathbf{v}_i(0)\cdot\sum_j \mathbf{v}_j(t)\right\rangle$ as shown in the linear-response theory by Kubo.[47] The Haven ratio is an indicator of the cooperativity in the ionic motions because it includes the cross term. Since the Haven ratio is known to be only slightly smaller than 1 in the silica rich region,[50,51] diffusive motion is a representative for the changes in the conductivity. The behavior of the original system mentioned above is useful to understand the modification by introducing pores.

In Fig. 2(a), the diffusion coefficients of Li ions thus determined by the Einstein equation are plotted against the density of the systems at 600, 700, and 800 K. As shown in this figure, the maximum of the diffusion coefficient is predicted at around ρ = 1.98, where the diffusion coefficient is more than one order higher than the original system at 600 K. The shape of the curves connecting different densities (porosities) slightly changes with temperature and this is mainly due to the larger temperature dependence of the diffusivity in the high density region. Note that the diffusion coefficient at 600 K of the original system shown in this figure is the upper limit value because temperature tends to increase slightly during the run because of the non-equilibrium nature of the system.

Temperature dependent diffusion coefficients in these systems are shown in Fig. 2(b). The solid line in this figure represents the approximate positions of the experimental values gathered in Ref. 37. The smaller temperature dependence is found in the porous systems. That is, the enhancement of the diffusivity is larger at lower temperatures and this fact is promising to use the porous system as high conductivity materials in the lower temperature region.

As shown in Eq. (6), similar behavior of the conductivity to the diffusion coefficient is naturally expected. The maximum of the conductivity and the smaller temperature dependence are commonly found in some composites of AgI and M_xO_y (=Al_2O_3, ZrO_2, and SiO_2) with different compositions and roles of interface regions suggested.[4] Comparable behaviors are also observed for nanocrystalline BaF_2 and CaF_2 and in BaF_2:CaF_2 composites.[6]

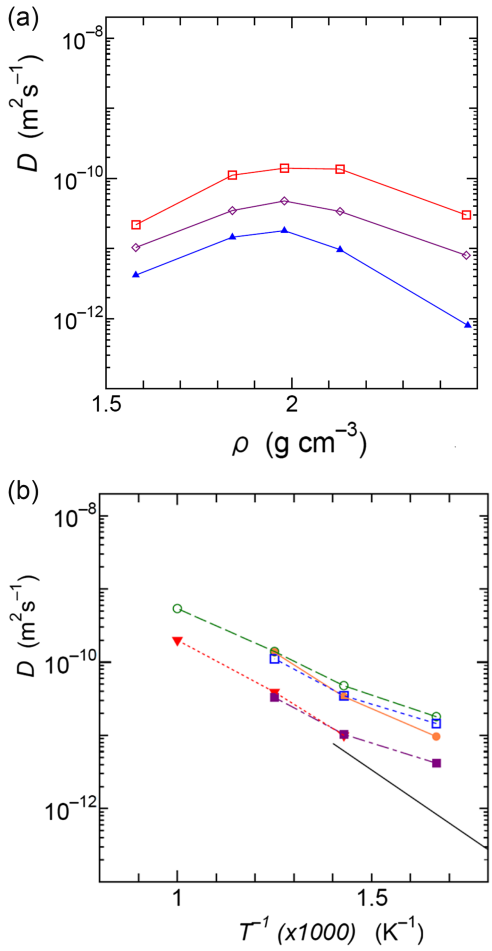

FIG. 2. (a) Diffusion coefficients of Li ions in porous lithium disilicate. The largest density (the right end point) corresponds to the original system before expansion. Blue triangles: 600 K, purple diamonds: 700 K, and red open squares: 800 K. The maximum is found at around ρ = 1.98 (in g cm^{-3}), where the diffusion coefficient is predicted to be one order higher than the original system. The enhancement is larger at lower temperatures. (b) Temperature dependence of diffusion coefficients of Li ions for each ρ value with some additional data points. Inverse triangles (red): ρ = 2.47, system in the glassy state without expansion. Filled circles (orange): ρ = 2.13, open circles (green): ρ = 1.98, open squares (blue): ρ = 1.84, and filled squares (purple): ρ = 1.58. The solid black line is the approximate position of experimental values for lithium disilicate glass gathered in Ref. 37.

C. Dynamical changes towards the maximum of the diffusion coefficient

In Figure 3, time dependence of the MSD of Li ions is shown for porous systems as well as that for the original system. In the porous systems, MSDs increased earlier time than that in the original system and the NCL region is shortened. The level of the MSD value is also affected by the density. Thus the change of the dynamics found in the diffusion coefficient starts at the early time region.

At the same time, in porous systems showing high-diffusivity of Li ions, levels of Si and O are found to be larger than the original system and no flat region of O atoms is observed after 1 ps. Therefore, motions of networks are

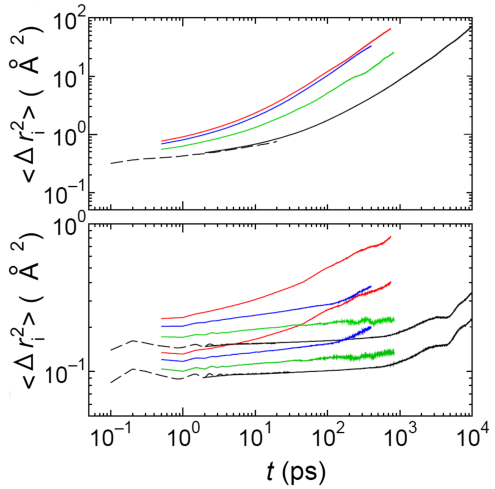

FIG. 3. Top: MSD of ions and atoms in lithium disilicate in porous systems at 800 K (upper curves). Upper panel: Li ions for ρ = 2.47 (black) (original), 2.30 (green), 2.13 (blue), and 1.98 (red) from lower to upper. The diffusivity of the system increases in this order. Bottom: MSD of Si (lower four curves in the beginning part) and O (upper four curves in the beginning part) of the same systems. The same color as that for MSD of Li ions is used for each atom. The long time data for ρ = 2.47, which were obtained by a larger time step (4 fs), are smoothly connected to those for short time scale (dashed curves) obtained by a smaller time step (1 fs).

non-negligible even at the short time region. This is a direct evidence to show that the enhancement of mobility of Li ions is accompanied with the loosening of cages.

In Fig. 3, long time data for ρ = 2.47, which were obtained by a larger time step (4 fs), are connected smoothly to those for short time data (dashed curves) obtained by a smaller time step (1 fs). Therefore, the choice of the time step here does not affect the argument in the present work.

D. Changes in the caging dynamics—Trajectories of ions and atoms

As discussed in Sec. III C, the change in MSD starting from the early time region suggests that the looser caging of Li ions than the original system can be a cause of a larger mobility of ions. This explanation is consistent to the trajectories shown in this section and topological analysis, which will be shown later.

In Figures 4(a) and 4(b), trajectories of Li ions, Si atoms, and O atoms at 600 K in original and porous lithium disilicate during 100 ps run are shown for a slice with a width of 10 Å of MD cell, respectively. The density of the porous system is ρ = 1.98, where the maximum of the diffusion coefficient at 600 K is found.

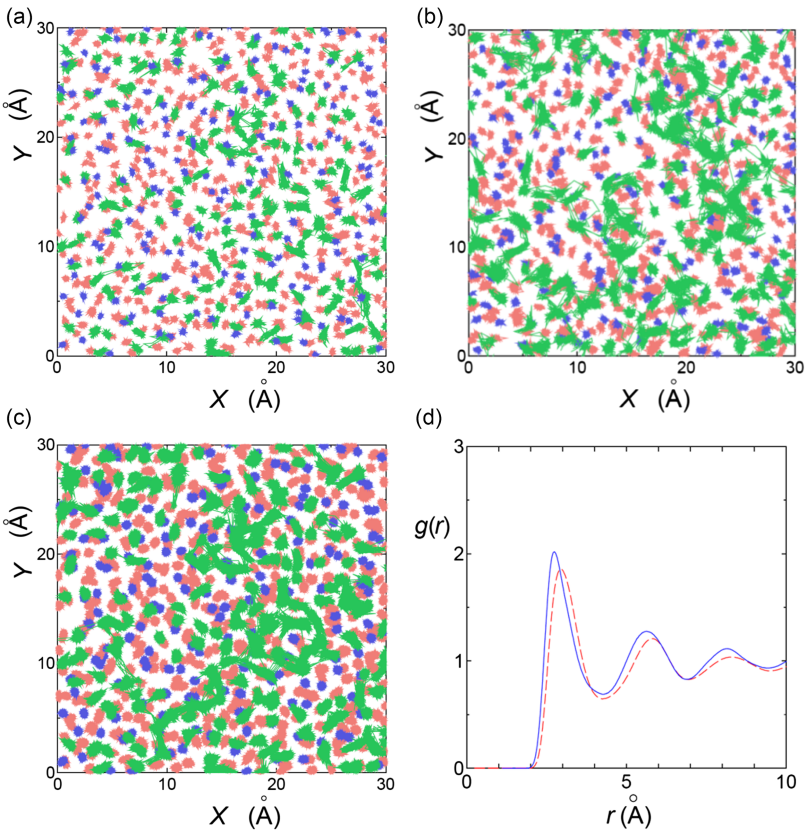

FIG. 4. (a) Trajectories of ions and atoms during 100 ps (100 000 steps) run of original $Li_2Si_2O_5$ glass at 600 K for a slice with a width of 10 Å of MD cell of the system. (b) Enhanced dynamics found in the trajectories of ions in porous lithium disilicate during 100 ps run near the maximum of the mobility at 600 K with ρ = 1.98. Green: Li ions, blue: Si atoms, and red: oxygen atoms. Not only motion of Li ions, mobility of O and Si atoms in the porous system is larger than the original system. (c) Trajectories of ions and atoms during 5 ns run of original $Li_2Si_2O_5$ glass at 600 K for a slice with a width of 10 Å of MD cell of the system, where the MSD (3 Å^2) of Li ions is comparable to the Li ions in (b). In each case, data are plotted with each 500 fs interval. Numbers of data points in (c) are larger than the other two cases because of longer time observation. (d) Comparison of the pair correlation function, g(r), of Li–Li in the original system at 600 K (blue solid curve) and that for ρ = 1.98 at 600 K (red dashed curve). Typical Li–Li distance in the system with the enhanced diffusion in (b) is longer than that in (a). Therefore, this enhancement is not caused by the formation of the high density region of Li ions.

Enhanced dynamics are observed in the bulk part and not necessarily remarkable at the boundary of the clear pores. They are accompanied with the larger motions of Si and O atoms than the original system as already mentioned. In the figure, ion channels are observed by the overlap of trajectories of Li ions with the enhanced diffusivity. Some ions are located for a long time, while fast ions form the channels. Thus the ionic motion is heterogeneous as known for the original system as well as other ionic systems.[16–18]

In Figure 4(c), trajectories for longer runs (5 ns) in original system are shown, where the MSD of Li ions is comparable to the value found in (b). In both (b) and (c), heterogeneous motions of Li ions are observed.

In Figure 4(d), pair correlation function g(r) of Li–Li pairs of the porous system (ρ = 1.98) at 600 K is compared with that in the original system. The peak positions of the first and second peaks shift toward right and peak heights become smaller by decreasing density. Usually, formation of the ion channel is observed in the region with high density of ions in the original system.[52] Therefore, one may expect that the formation of high density region of Li ions is a cause of the enhancement. However, this is not the case. Li ions in the porous system are more separated by decreasing density as shown in Figure 4(d). The results reveal that the enhanced dynamics discussed here is not caused by a formation of dense Li ion region.

E. The role of the caged particle dynamics in the enhancement of dynamics

In this section, we discuss the situation of caged particles in dynamics in glass forming ionic liquids and in lithium disilicate glasses. Note that there are some differences between the situations of ionic liquids and ionically conducting glasses. In the former, the ionic species are also the glass forming species, while in the latter, ionic species is still mobile in the glassy state.

In a previous work[31] for ionic liquid, 1-ethyl-3-methyl imidazolium nitrate (EMIM-NO_3), we have shown that the mobility of ions is closely related to both the change of the geometrical degree of freedom of coordination polyhedra and total number of bonds (including fictive ones for neighboring (contact) ions or atoms). Combination of these concepts can explain both characteristic temperatures, T_B and T_g, of the system.[53] A loss of geometrical degree of the freedom occurs with the closed packing of coordination polyhedra in a shell, while the saturation of the number of the constraints (bonds, contact ion pairs) is found near T_g, which is related to the concept of the rigidity percolation of (fictive) bonds.[31]

In the lithium silicate systems, LiO_x polyhedra and networks formed by SiO_4 polyhedra are mixing. For the structures at ρ = 1.98 at both temperatures, the coordination number of O around Si is 4 for ~100% of Si as found in the original disilicate glass. That is, SiO_4 units are kept unchanged while the N_V value of LiO_x structure changes gradually. Therefore, structural changes in the porous systems are characterized well by the latter. The length of Si–O bonds (in Å) is only slightly changed. That is, the distance 1.493–1.846 (the mean value is 1.638) is found for the original system, while 1.498–1.843 (the mean value is 1.652) is found for ρ = 1.98.

In Figure 5(a), distribution of coordination number N_v (number of O atoms around Li ion) is shown for each density of system at 800 K. Each distribution was obtained for an instantaneous structure after the quasi-equilibration of the system, for which the reproducibility and statistics are good enough for comparison of systems with different densities. In this figure, the position of the maximum of the peak is found at 5 before expansion of the system. The findings are comparable to the situation in lithium metasilicate, where the saturation of the total number of Li–O bonds and a comparable distribution were found,[29,30] near Tg, when the temperature of the system was decreased. The increase of the coordination number with decreasing temperature means that the coordination polyhedra are more overlapped to each other at lower temperatures. In the case of LiO_x polyhedra, sum of N_v values of all polyhedra corresponds to the total number of Li–O bonds. Therefore, this saturation means that the increasing overlapping of polyhedra is no more allowed. The peak position of the distribution shifts to 4 with decreasing density. This is shown in Figure 5(a). The deviation naturally resulted in the enhanced diffusion of Li ions and this trend is in accordance with the relation between the slowing down of the dynamics near T_g and the number of constraints clarified before.[29–31] The distribution patterns for 600 K (not shown) and 800 K are found to be almost the same.

The deformation of the coordination polyhedra is also affected by the N_b explained below. The geometrical degree of freedom, $F_{polyhedon}$,[28] changes by introducing pores as shown in Fig. 5(b). The degree is defined by $F_{polyhedon} = [(3N_v - 6) - N_b]$, where N_v is the number of vertices, that is, coordination number, and N_b is the number of bonds (contact ion pairs for ionic liquid and contact oxygen pairs for LiO_x structures). In the concept of deformation characterized by the $F_{polyhedon}$, effects of bond-bending constraints are included. The $F_{polyhedon}$ is 0 when $N_b = 3N_V - 6$, where 6 means the translational and rotational degrees of freedom of the polyhedron. In other words, N_b braces characterized by this equality are required to fix the shape of the polyhedron. Thus one needs to consider the change in N_b, which is relating to the mobility of the caged ions.[29–31]

Original structure at 600 K is shown in the top panel of Fig. 5(b) and the porous system with ρ = 1.98 (in g cm^{-3}) at the same temperature is shown in the bottom panel. In this figure, polyhedra with $N_b = 3N_V - 6$ are colored yellow, while those with $N_b < 3N_V - 6$ are colored green. Coordination polyhedra for the network part (SiO_4 units) are colored blue. With the expansion of the original system to this density, coordination polyhedra (yellow) with $N_b = 3N_V - 6$ decreased from 318 to 232 (0.73 times larger) and the floppy structure (green) with $N_b < 3N_v - 6$ increased from 370 to 420 (1.14 times larger), while the number of the structure with overconstraint ($N_b > 3N_v - 6$) was almost unchanged. Obviously, the number of polyhedra with a floppy mode ($N_b < 3N_V - 6$) having a looser caging increases by the expansion of the system. This change as well as that found in the coordination number of the cage of ions can be responsible for the changes in MSD. Thus the porous systems are characterized by the increase of the structure with a floppy mode as well as smaller coordination numbers. Therefore, similar concepts as used to characterize the glass transition in the ionic liquids are found

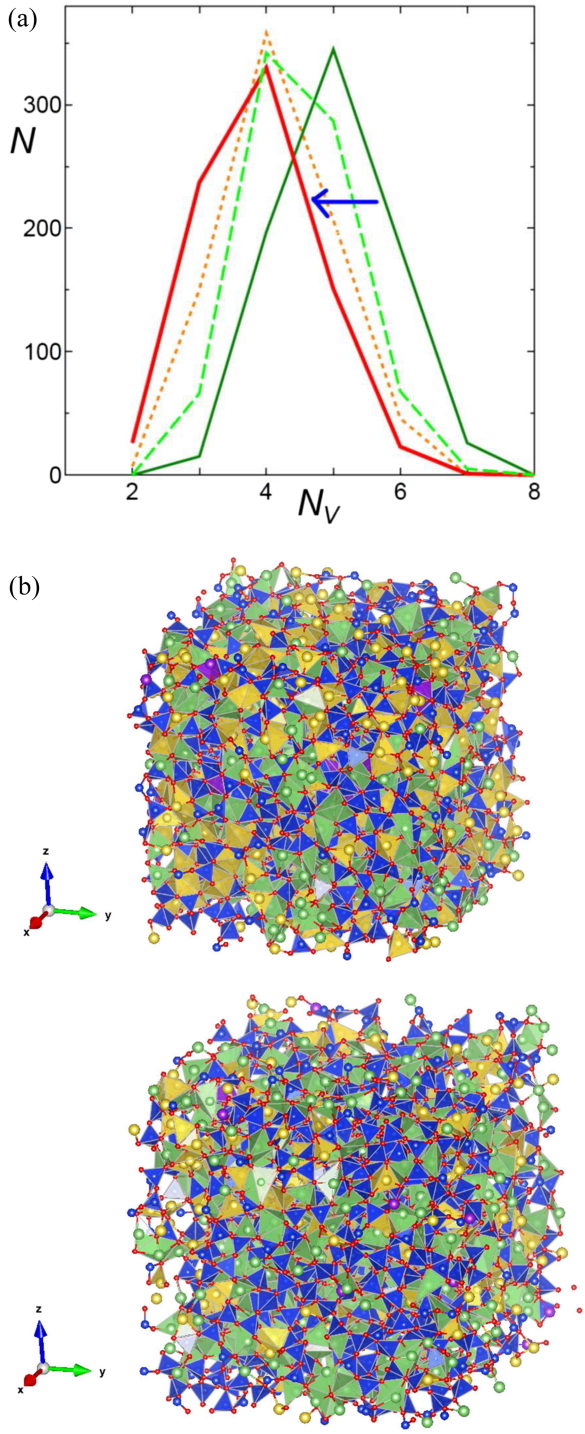

FIG. 5. Topological change of the coordination polyhedra (O atoms around Li ion) by introducing pores with decreasing density. (a) Changes of the distribution of coordination number at 800 K. Green (solid) line: for the original lithium disilicate glass. Pale green (dashed) line: for the porous system with ρ = 2.30, orange (dotted) line: for ρ = 2.13, and red (thick solid) line: for ρ = 1.98. An arrow (blue) in this figure means the trend with decreasing density. (b) Changes of the geometrical degree of freedom of the coordination polyhedra. Upper panel: structure before expansion at 600 K. The structure with $N_b = 3N_V - 6$ is shown in yellow. The structure $N_b < 3N_v - 6$ (structure with a floppy mode) is shown in green. SiO_4 units are shown in blue. Lower panel: the structure after expansion at 600 K, for which the largest diffusion coefficient was observed (ρ = 1.98). Colors are the same as those in the upper panel. By expansion, coordination polyhedra with $N_b = 3N_v - 6$ decreased from 318 to 232 and the floppy structure with $N_b < 3N_v - 6$ increased from 370 to 420. Here, the total number of Li ions (and hence coordination polyhedra around Li ions) is 768. The size of each figure in these panels is proportional to the system size, approximately.

to be applicable to characterize the conduction, that is, "caged ion dynamics" have important roles as in silicate glasses.[29,30]

F. Further decrease of the dynamics after the maximum

Decrease of the diffusion coefficient is found with the further decrease of the density (see Figure 2(a)). As shown in Figure 6, MSDs of Li ions, Si, and O atoms decrease and the NCL region of these species becomes longer again. Interestingly, this slowing down also starts from the early time region.

With a further expansion of the system, coordination number of the LiO_x structure tends to increase as shown in Figure 7(a). The trend observed in this figure qualitatively corresponds to the changes in the diffusivity of the system. That is, with increase in the coordination number, the mobility of ion decreases. The result suggests that a rearrangement of structure occurs after the formation of larger (the size is still in the nano-scale) voids.

G. Rearrangement of the coordination polyhedra with formation of voids

In Figure 7(b), the wire frame structure of the system with the largest mobility at 600 K is compared with other systems with smaller densities. In the system with the largest mobility, small pores are more homogeneously spreading over than the other systems. The total number of Li–O of the system changed from 2178 at ρ = 1.98 to 2181 at ρ = 1.85. That is, the number of Li–O bonds does not decrease with the expansion of the system. With further expansion of the system to ρ = 1.58, larger voids are formed as shown in the right panel. Further rearrangement of coordination polyhedra occurred and the rest part of the structures become more tightly packed one. The total number of Li–O bonds was found to increase to 2352 (after equilibration) in this case. The tightening naturally explains the decrease of the diffusion coefficient of ions after the maximum.

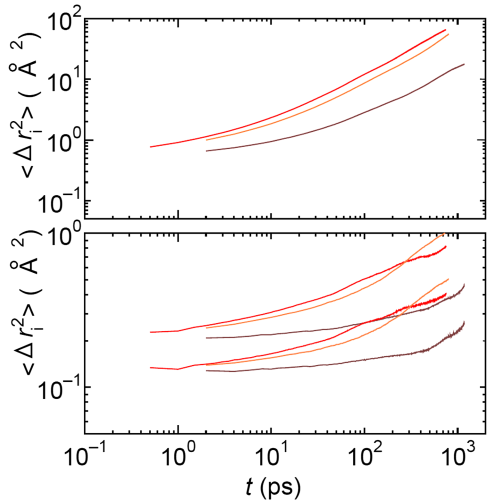

FIG. 6. Dependence of MSD on density (porosity) of $Li_2Si_2O_5$ systems at 800 K. Upper panel: Li ions for ρ = 1.98, 1.84, and 1.58 from upper to lower. The diffusivity of the system decreases in this order. Lower panel: Si and O atoms. Upper three curves are for O atoms and lower three curves are for Si atoms. Density is 1.98, 1.84, and 1.58 from upper to lower for each species.

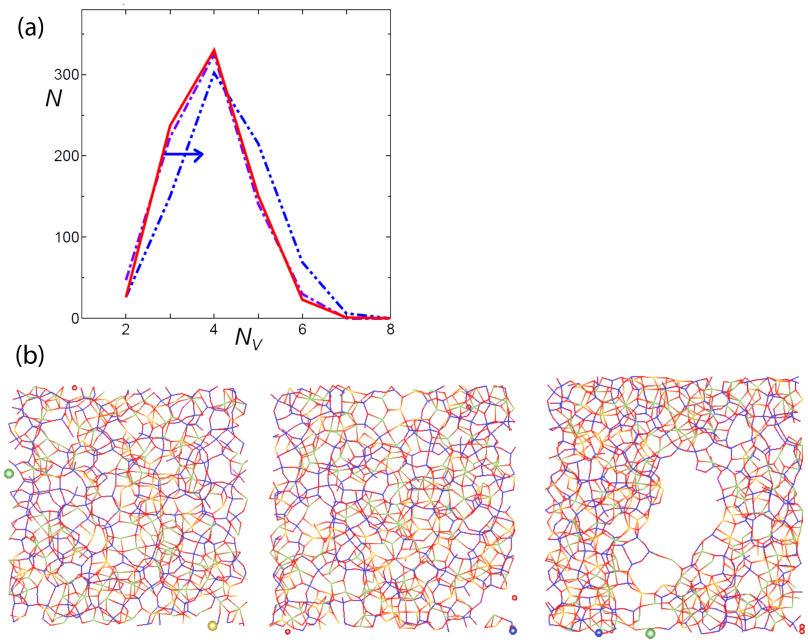

FIG. 7. (a) The dotted-dashed (purple), two dotted-dashed (blue) lines represent the distribution of the coordination number (N_v) of the LiO_x polyhedra for ρ = 1.84, ρ = 1.58 at 800 K. The arrow (blue) means the trend with the decreasing density. The distribution for ρ = 1.98 (a thick solid line, red) is shown again for the sake of comparison. (b) Topologies and location of voids for a slice with a width of 10 Å of MD cell. Wire frames representation for the Li–O and Si–O bonds is shown. Colors of bonds are the same as in Fig. 5(b). Some atoms without bonds within the slice are also shown. Left panel: ρ = 1.98, middle panel: ρ = 1.84, and right panel: ρ = 1.58. The system with ρ = 1.98 shows the largest diffusivity and the network looks rather homogeneous. It becomes more heterogeneous in the system with ρ = 1.84 with a formation of looser structures. Large voids (the longest diameter is ∼20 Å) are found in the right panel and other parts become closely packed again. In this figure, side length of each projection is proportional to the axis length of the system examined.

H. Formation of larger voids and rearrangement of structures

To clarify the relation between the formation of voids and the structures of coordination polyhedra (LiO_x), time dependent behavior of the system at ρ = 1.58 during the equilibration and further runs was visualized for the slice of MD cell.

In Figures 8(a)–8(d), coordination polyhedra of Li ion are shown in the interval of 400 ps (100 000 steps), where the polyhedra are colored by its coordination number. In (a), several sizes of small voids are formed by the expansion of the system. In (b), the distribution of the coordination number is wide. That is, both small coordination number (N_v = 2, ion colored by purple) and polyhedra with a large coordination number (N_v = 7, polyhedron colored by pink) are observed frequently. As shown in Figure 8(c), larger voids were formed in the local region with small coordination numbers found in (b). In Figure 8(d), the shapes and sizes of the voids are comparable to those in Figure 8(c), while the rearrangement of coordination polyhedra is still found as shown by the color change. Because the porosity of the system is a linear function of the density as shown in Eq. (2), the formation of the large void means the decrease of free space (small pores) in other parts. Therefore, the smaller pores found in (a) and (b) were not found here because of rearrangements of the rest part.

I. Relationships between structure and dynamics

Thus the loosening of the cage is considered to be the main factor to explain the enhancement of the dynamics observed in the porous materials. Concerning with these findings, some quantitative relations between the dynamics of ions and the changes in the coordination polyhedra were shown in previous works for lithium metasilicate glass.[29,30,54] It was also shown that the spectra obtained for fluctuation of N_v and N_b in the coordination polyhedra are closely related to those for the motion of caged ions in ionic liquid, EMIM(NO_3).[31] These observations are consistent to the results in the present work.

Further quantitative treatments of the dynamics are in planning and only the relationship between the dynamics of ions and its coordination number will be shown here.

In Fig. 9, partial MSD of Li ions is plotted for each N_V value at initial times t_0 for original and porous lithium disilicate systems (ρ = 1.98) at 700 K and 600 K. Here the partial MSD value for Li ions was obtained for 500 initial times covering 500 ps-1 ns of time windows in each case. As shown in Figs. 9(a) and 9(b), for the structure with a smaller N_v in the original system, the larger squared displacement of Li ions was found at around 1–4 ps. Jump motions of ions accompanied with the fluctuation of the coordination number started there. Initial increase of partial MSD depends on the coordination number N_V and it decreases in the order of 2 > 3 > 4 > 5 > 6 both at 600 and 700 K. Li ions surrounded by two or three oxygen atoms show large mobility during several ps. After the changing coordination number, behaviors are gradually averaged. While the partial MSDs in the case of N_V larger than 4 are small and small values continued for a long time. For the structure with N_V = 6, the value in the short time scale was larger than that for N_V = 5 and it decreased later. The value for N_V = 3 also shows the decreases at longer time scales. The difference in coordination number is larger at lower temperature in the original system.

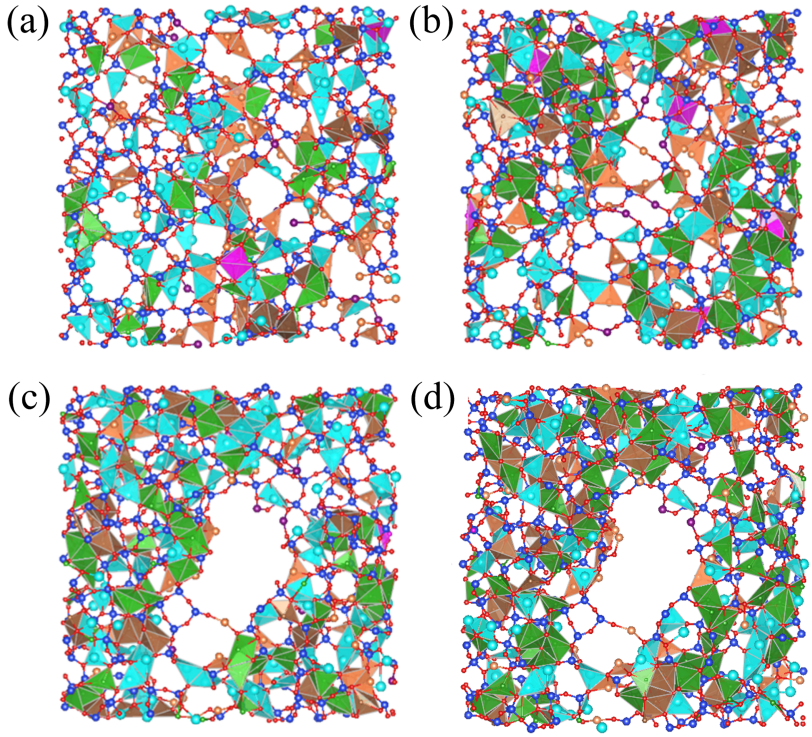

FIG. 8. Development of large void in the system at ρ = 1.58 with an elapse of time from (a) to (d), which is shown in the interval of 400 ps (100 000 steps) at 600 K for the slice of 10 Å. Each polyhedron is colored by its coordination number, N_v. Orange:3, pale blue:4, green:5, brown:6, pink:7. Li colored by purple is for the structure with N_v = 2. In (a), many small pores exist in the system. In (b), the region containing the polyhedra with small coordination number of Li developed and many small pores are observed there. The system also shows some structures with a large coordination number. (c) Large voids were formed with the rearrangement of polyhedra and network formed by SiO_4 units. (d) The shapes and sizes of the voids are comparable to (c), while the rearrangement of coordination polyhedra is found as shown by the color change. The situation in (d) corresponds to the right panel in Fig. 7(b).

As shown in Figs. 9(c) and 9(d), in the case of porous system with ρ = 1.98, the initial increases of the partial MSD with the fluctuation of the coordination number are observed much earlier time (~1 ps) as already discussed. The relation between the coordination number and the partial MSD is lost rapidly in the porous system. Still, a clear relationship between the coordination number and MSD exists, but the coordination number alone is not enough to explain the behavior of ions in porous materials. One needs to consider the changes in N_b values and changes in the time scale of NCL region at the same time.

J. Relation between stress in the system and dynamics

Because the porous system in the present work was prepared by the expansion of the original system, observed

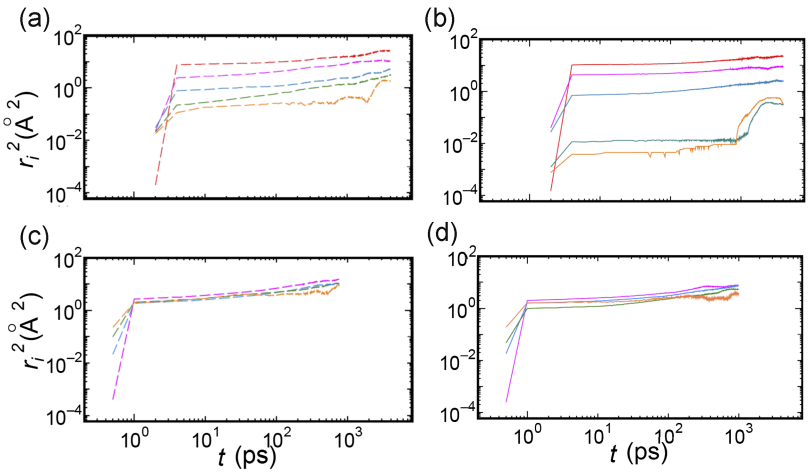

FIG. 9. Partial MSDs of Li ions classified by its coordination number (N_V) at an initial time. These values are averaged for 500-1000 initial times. (a) Original system at 700 K. N_v changes from 2 to 6 (from upper to lower at the right part). Red: N_v = 2, pink: N_v = 3, blue: N_v = 4, green: N_v = 5, orange: N_v = 6. (b) Original system at 600 K. N_v changes from 2 to 6. The same colors as in (a) are used. (c) Porous system with ρ = 1.98 at 700 K. N_v changes from 3 to 6 (from lower to upper at the beginning). (d) Porous system with ρ = 1.98 at 600 K. N_v changes as a similar manner as in (c) at the beginning. Structures with N_v = 7 are found, but result for this case is omitted here because the result is not statistically meaningful.

enhancement may be correlated with the residual stress in the system. Therefore, the relation between such mechanical properties and dynamics in porous systems is worthy to examine.

From the virial theorem, pressure of the system is defined as follows:[55,56]

$$P = \frac{1}{V}Nk_BT + \frac{1}{3v}\left\langle \sum_{i=1}^{N} \mathbf{r}_i \cdot \mathbf{F}_i \right\rangle, \tag{7}$$

where $\mathbf{F}_i$ is a total force acting on the i-th particle (atom or ion).

As shown in Eq. (7), pressure of the system is a function of the position of the particles on the potential surface and each component of pressure tensor of the system is also a function of it. In the case of MD using the pair potential $u(r_{ij})$, P can be obtained from the following form:

$$\begin{aligned} P &= \tfrac{1}{V}Nk_BT - \tfrac{1}{3v}\left\langle \sum_{i=1}^{N}\sum_{j>i}^{N} r_{ij}\frac{d}{dr_{ij}}u(r_{ij}) \right\rangle, \\ r_{ij} &= \left|\mathbf{r}_i - \mathbf{r}_j\right|. \end{aligned} \tag{7'}$$

We can explain the nanoscopic origin of the pressure and related residual stress in the system not only by the changes in the distance among particles but also by those in the structures of polyhedra (and those in further shells).

In Table I, pressure of each system during the *NVE* run after the quasi-equilibration was shown. The value shows the minimum at around ρ = 1.84. The position is near the maximum of the diffusion coefficient of Li ions in the system. In the case of the lowest density (ρ = 1.58), the change of the pressure was observed during the formation of larger voids in *NVE*. This means that the further rearrangement of the structure was caused by the stress relaxation in the system. Even after the following *NPT* run with an increase in the pressure (to ∼0 atm), larger voids formed are still found even after 1 000 000 steps.

On the other hand, when *NPT* run was performed after the *NVE* run in the system (ρ = 1.98), the system gradually shrank to ρ = 2.44 and the pressure of the system decreased to ∼0 katm within 150 ps at 600 K. Recently, Wang *et al.* have examined the stress-strain curve of several systems including sodium silicate using MD simulations and argued that the silicate system shows the ductile behaviors[57] and then fracture is observed. Our results are consistent to theirs. That is, in medium density region, the system shows an elastic property. Therefore, the observed structural change is a microscopic origin of the residual stress in the system and it accompanies with the enhancement of the dynamics. In a macroscopic point of view, this statement seems to be equivalent to say that the enhancement is caused by the strain of the system.

TABLE I. Pressures of systems during the *NVE* run after the quasi-equilibration using the *NVT* condition. The values in porous systems are negative and show the minimum at around ρ = 1.84.

ρ in g cm^{-3}	P in katm (1 atm = 101 325 Pa)
2.47	0.002
2.13	−51.12
1.98	−59.22
1.84	−66.00
1.58[a]	−59.25
1.58	−31.32

[a]The system before the forming of larger voids.

K. Percolative aspect for the dynamics

Asymmetry of the curve for the diffusion coefficient against the density plot (Fig. 2(a)) is clearer at lower temperatures and dynamics are more enhanced in a longer time scale in some cases. These findings suggest that the existence of another factor (or factors) plays the roles to determine diffusivity. One of the possible explanations is concerning with the geometrical changes of the trajectories and related jump paths. In several nano-porous or meso-porous systems reported in the literatures, the maximum of the transport properties observed in experiments is often explained[11] by the percolation theory.[58] Since the slow dynamics in the original densely packed system is affected by the strong back correlated motions of ions, the geometrical characteristics of paths are a non-negligible factor.

Actually, geometric correlations of trajectories with strong back correlations contributing to the slowing down of the dynamics near Tg of the original system are changed by introducing pores considerably. Thus the changes of geometry of the paths and walks of ions affect the dynamics, although the existence of the maximum is already explained by the changes of short time caging dynamics.

IV. CONCLUSIONS

In porous lithium disilicate system, enhancement of the diffusion coefficient having the maximum in the medium density region is predicted by the molecular dynamics simulation in the *NVE* condition. The porous model system for MD is prepared by the expansion of the system started from the glassy lithium disilicate, so that the effect of disorder (difference of ionics in crystal and glass) was separated beforehand. The enhancement of the diffusive motion of Li ions is found to occur not only at the boundary of pores but also in the bulk part of the systems. The enhancement of the diffusion coefficient (and hence that of the conductivity) starts from an early time (NCL) region of the mean squared displacement and it means that the loosening of the cage contributes to the enhancement. Changes found in the distribution of the coordination number and in the geometrical degree of freedom of coordination polyhedra (formed by oxygen atoms around Li ions) are consistent to this view.

Decrease of the coordination number in LiOx polyhedra is found before the maximum of the diffusivity, while its increase is observed after that. The latter change is accompanied with the rearrangement of networks after the formation of larger voids. Therefore, the maximum is explained by the change of the caging as a first approximation and we found that the existence of the larger void is not necessarily effective for the enhancement of dynamics. These behaviors are closely related to the residual stress in the system and further study of the structures and stress in related composites will be interesting.

For the dynamics of ions in the glassy lithium disilicate system, change in the slope of the MSD in the power law region contributes to the slowing down of the dynamics considerably

and this situation is changed by introducing pores. Thus the geometrical characteristics of trajectories also contribute to the dynamics, although the maximum already exists in the early time region. As shown in the present paper, a guide how to distinguish and control factors to affect dynamics is given and MD simulation is shown to be beneficial to examine and predict the properties of porous materials.

ACKNOWLEDGMENTS

This work is stimulated by the fruitful collaboration with K. L. Ngai and C. León during the project of writing book for Ionics. The author would like to thank them.

[1]K. Kanamura, N. Akutagawa, and K. Dokko, J. Power Sources **146**, 86 (2005).
[2]K. Dokko, N. Akutagawa, Y. Isshiki, K. Hoshina, and K. Kanamura, Solid State Ionics **176**, 2345 (2005).
[3]M. Hara, H. Nakano, K. Dokko, S. Okuda, A. Kaeriyama, and K. Kanamura, J. Power Sources **189**, 485 (2009).
[4]K. Tadanaga, K. Imai, M. Tatsumisago, and T. Minami, J. Electrochem. Soc. **149**, A773 (2002).
[5]H. Yamada, A. J. Bhattacharyya, and J. Maier, Adv. Funct. Mater. **16**, 525 (2006).
[6]B. Ruprecht, M. Wilkening, S. Steuernagel, and P. Heitjans, J. Mater. Chem. **18**, 5412 (2008).
[7]J. Maier and J. Phys, Chem. Solids. **46**, 309 (1985).
[8]J. Maier, Mater. Res. Bull. **20**, 383 (1985).
[9]C. C. Liang, J. Electrochem. Soc. **120**, 1289 (1973).
[10]T. Jow and J. B. Wagner, Jr., J. Electrochem. Soc. **126**, 1963 (1979).
[11]S. Fujitsu, M. Miyayama, K. Koumoto, H. Yanagida, and T. Kanazawa, J. Mater. Sci. **20**, 2103 (1985).
[12]M. Sillassen, P. Eklund, N. Pryds, E. Johnson, U. Helmersson, and J. Bøttiger, Adv. Funct. Mater. **20**, 2071 (2010).
[13]A. Ohtomo, D. A. Muller, J. L. Grazul, and H. Y. Hwang, Nature **419**, 378 (2002).
[14]S. Thiel, G. Hammerl, A. Schmehl, C. W. Schneider, and J. Mannhart, Science **313**, 1942 (2006).
[15]J. Habasaki, C. León, K. L. Ngai, *Dynamics of Glassy, Crystalline and Liquid Ionic Conductors, Experiments, Theories, Simulations* (Springer, 2016), available at http://www.springer.com/jp/book/9783319423890.
[16]J. Habasaki, I. Okada, and Y. Hiwatari, Phys. Rev. E **52**, 2681 (1995).
[17]J. Habasaki, I. Okada, and Y. Hiwatari, Phys. Rev. B **55**, 6309 (1997).
[18]J. Habasaki, K. L. Ngai, and Y. Hiwatari, Phys. Rev. E **66**, 021205 (2002).
[19]L. G. V. Gonçalves and J. P. Rino, J. Non-Cryst. Solids **402**, 91 (2014).
[20]H. Lammert and A. Heuer, Phys. Rev. Lett. **104**, 125901 (2010).
[21]C. Mueller, E. Zienicke, S. Adams, J. Habasaki, and P. Maass, Phys. Rev. B **75**, 014203 (2007).
[22]J. Habasaki and K. L. Ngai, J. Electroceram. **34**, 43 (2015).
[23]R. A. Montani, C. Balbuena, and M. A. Frechero, Solid State Ionics **209-210**, 5 (2012).
[24]J. Habasaki and I. Okada, Mol. Simul. **9**, 319 (1992).
[25]R. Küchler, O. Kanert, T. Vereget, and H. Jain, J. Non-Cryst. Solids **353**, 3940 (2007).
[26]A. M. Glass, K. Nassau, and T. J. Negran, J. Appl. Phys. **49**, 4808 (1978).
[27]T. Minami, Y. Takuma, and M. Tanaka, J. Electrochem. Soc. **124**, 1659 (1977).
[28]A. L. Loeb, *Space Structures* (Addison-Wesley,1976; Birkhäuser, Boston, 1991).
[29]J. Habasaki, I. Okada and Y. Hiwatari, in *Molecular Dynamics Simulations*, Springer Series in Solid-State Science Vol. 103, edited by F. Yonezawa (Springer, 1992), pp. 98–107.
[30]J. Habasaki, Mol. Phys. **70**, 513 (1990).
[31]J. Habasaki and K. L. Ngai, J. Chem. Phys. **142**, 164501 (2015).
[32]J. Kieffer and C. A. Angell, J. Non-Cryst. Solids **106**, 336 (1988).
[33]A. Nakano, L. Bi, R. K. Kalia, and P. Vashishta, Phys. Rev. B **49**, 9441 (1994).
[34]T. L. Gilbert, J. Chem. Phys. **49**, 2640 (1968).
[35]Y. Ida, Phys. Earth Planet. Inter. **13**, 97 (1976).
[36]J. Habasaki and K. L. Ngai, J. Chem. Phys. **139**, 064503 (2013).
[37]M. L. F. Nascimento, V. M. Fokin, E. D. Zanotto, and A. S. Abyzov, J. Phys. Chem. **135**, 194703 (2011).
[38]J. V. L. Beckers and S. W. De Leeuw, J. Non-Cryst. Solids **261**, 87 (2000).
[39]S. Bhattacharya and J. Kieffer, J. Phys. Chem. C **112**, 1764 (2008).
[40]J. Habasaki and M. Ishikawa, Phys. Chem. Chem. Phys. **16**, 24000 (2014).
[41]J. M. Rimsza and J. Du, J. Am. Ceram. Soc. **97**, 772 (2014).
[42]R. R. Shaw and D. R. Uhlmann, J. Non-Cryst. Solids **1**, 474 (1969) and references therein.
[43]The method is taking into account the atomic volumes and any nearest-neighbor intersections (by using the CrystalMaker®).
[44]B. Mandelbrot, Science **156**, 636 (1967).
[45]The system has different length scale regions so that it shows multifractal nature. In that case, different fractal dimensions of the random walk are found in each length scale region and two different fractal dimension of the random walk (d_{w_1} and d_{w_2} for short and long length scale regions) are found. The value found in the power law regions is for the mean behavior of the heterogeneous dynamics.
[46]A. Einstein, *Investigations on the Theory of Brownian Motion* (Dover, New York, 1956).
[47]R. Kubo, J. Phys. Soc. Jpn. **12**, 570 (1957).
[48]T. Odagaki and M. Lax, Phys. Rev. B **24**, 5284 (1981).
[49]Y. Haven and B. Verkerk, Phys. Chem. Glasses **6**, 38 (1965).
[50]G. E. Murch, Solid State Ionics **7**, 177 (1982).
[51]J. O. Isard, J. Non-Cryst. Solids **246**, 16 (1999).
[52]G. N. Greaves, *NATO ASI Series* (Springer, 1994), Vol. 418, pp. 87–122.
[53]K. L. Ngai and J. Habasaki, J. Chem. Phys. **141**, 114502 (2014).
[54]J. Habasaki, Z. Naturforsch., A: Phys. Sci. **46**, 616 (1991).
[55]R. J. E. Clausius, Philos. Mag. Ser. 4 **40**, 122 (1870), available at http://www.tandfonline.com/doi/abs/10.1080/14786447008640370.
[56]J. C. Maxwell, Trans. - R. Soc. Edinburgh **26**, 1 (1870).
[57]B. Wang, Y. Yu, M. Wang, J. C. Mauro, and M. Bauch, Phys. Rev. B **93**, 064202 (2016).
[58]W. Dieterich, O. Dürr, P. Pendzig, A. Bunde, and A. Nitzan, Physica A **15**, 229–237 (1999).